Paper:

Observer-Based Piecewise Multi-Linear Controller Designs for Nonlinear Systems Using Feedback and Observer Linearizations

Tadanari Taniguchi* **and Michio Sugeno****

*Tokai University
4-1-1 Kitakaname, Hiratsuka, Kanagawa 259-1292, Japan
E-mail: taniguchi@tokai-u.jp
**Tokyo Institute of Technology
4259 Nagatsuta-cho, Midori-ku, Yokohama, Kanagawa 226-8503, Japan
[Received June 14, 2019; accepted August 20, 2019]

This paper proposes observer-based piecewise multi-linear controllers for nonlinear systems using feedback and observer linearizations. The piecewise model is a nonlinear approximation and fully parametric. Feedback linearizations are applied to stabilize the piecewise multi-linear control system. Furthermore, observer linearizations are more conservative in modeling errors compared with feedback linearizations. In this paper, we propose robust observer designs for piecewise multi-linear systems. Moreover, we design piecewise multi-linear controllers that combine the robust observer with various performance such as a regulator and tracking controller. These design methods realize a separation principle that allows an observer and a regulator to be designed separately. Examples are demonstrated through computer simulation to confirm the feasibility of our proposals.

Keywords: observer-based controller, piecewise multi-linear model, feedback linearization, observer linearization problem

1. Introduction

Piecewise control systems, which are nonlinear controls, have been widely studied. They are classified into piecewise linear and piecewise nonlinear systems. Piecewise linear (PL) systems, which are fully parametric, have been intensively studied in relation to nonlinear systems [1–4]. The piecewise linear approximation has general approximation capability for nonlinear functions with a given precision. The parametric piecewise approximation of nonlinear control systems is promising for constructing a system model.

A piecewise multi-linear (PML) approximation was proposed in [5]. The PML approximation also has general approximation capability for nonlinear functions with a given precision. The PML model is a piecewise nonlinear systems. A multi-linear function as a basis of PML approximation is (as a nonlinear function) the second simplest one after a linear function. The PML model has the following features: 1) It is derived from fuzzy if-then rules with singleton consequents; 2) It is built on piecewise hyper-cubes partitioned in the state space; 3) It has general approximation capability for nonlinear systems; 4) It is a piecewise nonlinear model, the second simplest after a PL model; 5) It is continuous and fully parametric. So far, we have provided the necessary and sufficient conditions for the stability of PML systems with respect to Lyapunov functions in the two dimensional case [6], where membership functions are fully considered. As the stabilizing conditions are represented by bilinear matrix inequalities [7], a long computing time is required to obtain a stabilizing controller. To overcome this drawback, we derived the stabilizing conditions [8] based on full-state feedback linearization approaches. In the PML modeling method, only partial knowledge of vertices in piecewise regions is necessary not the overall knowledge of an objective plant. The control system is applicable to a wider class of nonlinear systems compared with conventional feedback linearization.

This paper deals with observer-based PML controller designs for nonlinear systems via observer linearization. We proposed some observer design methods for piecewise systems in [9] and [10]. The paper [11] dealt with the necessary and sufficient conditions for observer linearization and showed that a PML model-based linearized observer could be applied to a wider system compared with the conventional one. Observer linearizations are more conservative in modeling errors compared with feedback linearizations. In this paper, we propose robust observer designs for piecewise multi-linear systems. In addition, we design piecewise multi-linear controllers that combines the robust observer with various performance such as a regulator and a tracking controller. These design methods realize a separation principle that allows observers and controllers to be designed separately. Examples are demonstrated through computer simulation to confirm the feasibility of our proposals.

2. Canonical Form of PML Models

We introduce the PML models proposed in [5]. For $x \in R_{\sigma_1 \ldots \sigma_n}$, the PML model (1) is constructed from the vectors $d(\sigma_1,\ldots,\sigma_n)$, $f(\sigma_1,\ldots,\sigma_n)$, $g(\sigma_1,\ldots,\sigma_n)$, and $h(\sigma_1,\ldots,\sigma_n)$.

$$\begin{cases} \dot{x} = f + gu, \\ \qquad\qquad \cdots\cdots\cdots\cdots \\ y = h, \end{cases} \quad (1)$$

where $x \in R^n$, $f \in R^n$, $g \in R^{n\times m}$, $u \in R^m$, $y \in R^p$, and $h \in R^p$,

$$f = \sum_{i_1=\sigma_1}^{\sigma_1+1} \omega_1^{i_1}(x_1) \cdots \sum_{i_n=\sigma_n}^{\sigma_n+1} \omega_n^{i_n}(x_n) f(i_1,\ldots,i_n),$$

$$g = \sum_{i_1=\sigma_1}^{\sigma_1+1} \omega_1^{i_1}(x_1) \cdots \sum_{i_n=\sigma_n}^{\sigma_n+1} \omega_n^{i_n}(x_n) g(i_1,\ldots,i_n),$$

$$h = \sum_{i_1=\sigma_1}^{\sigma_1+1} \omega_1^{i_1}(x_1) \cdots \sum_{i_n=\sigma_n}^{\sigma_n+1} \omega_n^{i_n}(x_n) h(i_1,\ldots,i_n),$$

$$x = \sum_{i_1=\sigma_1}^{\sigma_1+1} \omega_1^{i_1}(x_1) \cdots \sum_{i_n=\sigma_n}^{\sigma_n+1} \omega_n^{i_n}(x_n) d(i_1,\ldots,i_n),$$

$$\omega_j^{\sigma_j}(x_j) = \frac{d_j(\sigma_j+1) - x_j}{d_j(\sigma_j+1) - d_j(\sigma_j)},$$

$$\omega_j^{\sigma_j+1}(x_j) = \frac{x_j - d_j(\sigma_j)}{d_j(\sigma_j+1) - d_j(\sigma_j)},$$

$j = 1,\ldots,n$ and $\omega_j^i(x_j) \in [0,\ 1]$. Here, we assume $f(0,0) = 0$ and $d(0,0) = 0$ to guarantee $\dot{x} = 0$ for $x = 0$. **Fig. 1** shows a piecewise region of f in the two dimensional case.

A vector $d(\sigma_1,\ldots,\sigma_n)$ and rectangle $R_{\sigma_1\ldots\sigma_n}$ are defined, respectively, in n-dimensional space as $d(\sigma_1,\ldots,\sigma_n) \equiv (d_1(\sigma_1),\ldots,d_n(\sigma_n))^T$ and

$$R_{\sigma_1\ldots\sigma_n} \equiv [d_1(\sigma_1), d_1(\sigma_1+1)] \times [d_2(\sigma_2), d_2(\sigma_2+1)] \cdots \times [d_n(\sigma_n), d_n(\sigma_n+1)],$$

where

$$x_1 \in [d_1(\sigma_1),\ d_1(\sigma_1+1)],$$

$$x_2 \in [d_2(\sigma_2),\ d_2(\sigma_2+1)],$$

$$\vdots$$

$$x_n \in [d_n(\sigma_n),\ d_n(\sigma_n+1)],$$

σ_i is an integer: $-\infty < \sigma_i < \infty$ where $d_i(\sigma_i) < d_i(\sigma_i+1)$, $d(0) \equiv (d_1(0), d_2(0), \ldots, d_n(0))^T$, and $i = 1,2,\ldots,n$. The superscript ^{T} denotes a *transpose* operation. The vectors $f(\sigma_1,\ldots,\sigma_n)$, $g(\sigma_1,\ldots,\sigma_n)$, and $h(\sigma_1,\ldots,\sigma_n)$ correspond to the vector $d(\sigma_1,\ldots,\sigma_n)$ as

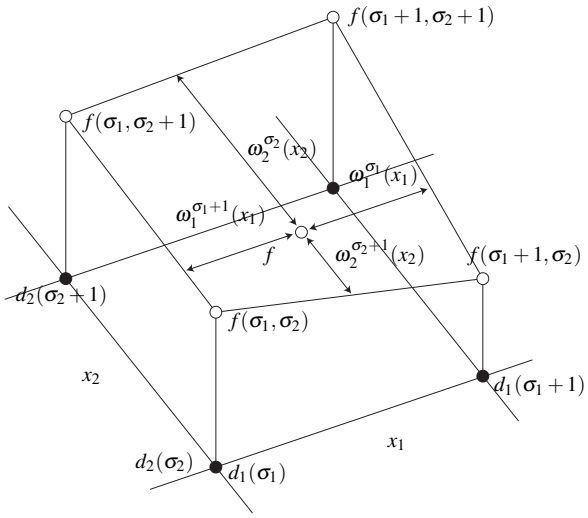

Fig. 1. Piecewise region of f in the two dimensional case.

$$f(\sigma_1,\ldots,\sigma_n) \equiv \begin{pmatrix} f_1(d_1(\sigma_1),\ldots,d_n(\sigma_n)) \\ \vdots \\ f_n(d_1(\sigma_1),\ldots,d_n(\sigma_n)) \end{pmatrix},$$

$$g(\sigma_1,\ldots,\sigma_n) \equiv \begin{pmatrix} g_1(d_1(\sigma_1),\ldots,d_n(\sigma_n)) \\ \vdots \\ g_n(d_1(\sigma_1),\ldots,d_n(\sigma_n)) \end{pmatrix},$$

$$h(\sigma_1,\ldots,\sigma_n) \equiv \begin{pmatrix} h_1(d_1(\sigma_1),\ldots,d_n(\sigma_n)) \\ \vdots \\ h_p(d_1(\sigma_1),\ldots,d_n(\sigma_n)) \end{pmatrix}.$$

The overall PML model is obtained automatically when all the vertices of the vectors d, f, g, and h are assigned. **Tables 1–4** show the values of the vectors d, f, g, and h in the two dimensional case. Note that the piecewise model can be constructed with only the vertex values of the rectangle regions without the model dynamics information. In our method, the piecewise model and controller can be represented as lookup tables (LUTs) and the dynamics is constructed as an interpolation of the vertices in the LUTs.

3. Regulator and Observer Designs for PML Systems

3.1. PML Controller

Consider the PML system (1), where f, g, and h are assumed to be sufficiently smooth in a domain $D \subset R^n$. The mappings $f : D \to R^n$ and $g : D \to R^n$ are called vector fields on D.

We show a feedback linearizing controller [12] for the PML systems using an input-output feedback lineariza-

Table 1. Vertex values of $d(i_1,i_2)$ in the two dimensional case.

$x_2 \setminus x_1$	$\cdots$	$d_1(\sigma_1)$	$d_1(\sigma_1+1)$	$\cdots$
$\vdots$		$\vdots$	$\vdots$	
$d_2(\sigma_2)$	$\cdots$	$d(\sigma_1,\sigma_2)$	$d(\sigma_1+1,\sigma_2)$	$\cdots$
$d_2(\sigma_2+1)$	$\cdots$	$d(\sigma_1,\sigma_2+1)$	$d(\sigma_1+1,\sigma_2+1)$	$\cdots$
$\vdots$		$\vdots$	$\vdots$	

Table 2. Vertex values of $f(i_1,i_2)$ in the two dimensional case.

$x_2 \setminus x_1$	$\cdots$	$d_1(\sigma_1)$	$d_1(\sigma_1+1)$	$\cdots$
$\vdots$		$\vdots$	$\vdots$	
$d_2(\sigma_2)$	$\cdots$	$f(\sigma_1,\sigma_2)$	$f(\sigma_1+1,\sigma_2)$	$\cdots$
$d_2(\sigma_2+1)$	$\cdots$	$f(\sigma_1,\sigma_2+1)$	$f(\sigma_1+1,\sigma_2+1)$	$\cdots$
$\vdots$		$\vdots$	$\vdots$	

tion [13]. The derivative $\dot{y}$ is given by

$$\dot{y} = \frac{\partial h}{\partial x}\{f+gu\} = L_f h + L_g h u,$$

where

$$\frac{\partial h}{\partial x_1} = \sum_{i_2=\sigma_2}^{\sigma_2+1} \omega_2^{i_2}(x_2) \cdots \sum_{i_n=\sigma_n}^{\sigma_n+1} \omega_n^{i_n}(x_n) \times \frac{h(\sigma_1+1,i_2,\ldots,i_n) - h(\sigma_1,i_2,\ldots,i_n)}{d_1(\sigma_1+1) - d_1(\sigma_1)},$$

$$\frac{\partial h}{\partial x_2} = \sum_{i_1=\sigma_1}^{\sigma_1+1} \omega_1^{i_1}(x_1) \sum_{i_3=\sigma_3}^{\sigma_3+1} \omega_1^{i_3}(x_3) \cdots \sum_{i_n=\sigma_n}^{\sigma_n+1} \omega_n^{i_n}(x_n) \times \frac{h(i_1,\sigma_2+1,i_3,\ldots,i_n) - h(i_1,\sigma_2,i_3,\ldots,i_n)}{d_2(\sigma_2+1) - d_2(\sigma_2)},$$

$$\vdots$$

$$\frac{\partial h}{\partial x_n} = \sum_{i_1=\sigma_1}^{\sigma_1+1} \omega_1^{i_1}(x_1) \cdots \sum_{i_{n-1}=\sigma_{n-1}}^{\sigma_{n-1}+1} \omega_{n-1}^{i_{n-1}}(x_{n-1}) \times \frac{h(i_1,\ldots,i_{n-1},\sigma_n+1) - h(i_1,\ldots,i_{n-1},\sigma_n)}{d_n(\sigma_n+1) - d_n(\sigma_n)}.$$

If $L_g h = 0$, then $\dot{y} = L_f h$ is independent of u. We continue to calculate the second derivative of y, denoted by $y^{(2)}$ and then we obtain

$$y^{(2)} = \frac{\partial\{L_f h\}}{\partial x}(f+gu) = L_f^2 h + L_g L_f h u.$$

Once again, if $L_g L_f h = 0$, then $y^{(2)} = L_f^2 h$ is independent of u. Repeating this process, we observe that, if h satisfies

$$L_g L_f^i h = 0, i = 0,1,\ldots,\rho-2,$$
$$L_g L_f^{\rho-1} h \neq 0,$$

then u does not appear in the equations of $y, \dot{y}, \ldots, y^{(\rho-1)}$ and appears in the equation of $y^{(\rho)}$ with a nonzero coefficient:

$$y^{(\rho)} = L_f^\rho h + L_g L_f^{\rho-1} h u.$$

The foregoing equation shows that the system is input-output linearizable, as the state feedback control

$$u = \frac{-L_f^\rho h + v}{L_g L_f^{\rho-1} h}$$

reduces the input-output map to $y^{(\rho)} = v$, which is a chain of ρ integrators. In this case, the integer ρ is called the relative degree of the system. The relative degree is derived using the following definition [14]:

Definition 3.1: The nonlinear system is said to have a relative degree ρ, $1 \leq \rho \leq n$, in a region $D_0 \subset D$ if

$$\begin{cases} L_g L_f^i h = 0, \ i = 0,1,\ldots,\rho-2 \\ L_g L_f^{\rho-1} h \neq 0, \end{cases} \quad \ldots\ldots (2)$$

for all $x \in D_0$.

The input-output linearized system can be formulated as

$$\begin{cases} \dot{\xi} = A\xi + Bv, \\ y = C\xi, \end{cases} \quad \ldots\ldots\ldots\ldots (3)$$

where $\xi \in \Re^\rho$, and

$$A = \begin{pmatrix} 0 & 1 & 0 & \cdots & 0 \\ 0 & 0 & 1 & \ddots & \vdots \\ \vdots & \vdots & \ddots & \ddots & 0 \\ 0 & 0 & \cdots & 0 & 1 \\ 0 & 0 & \cdots & 0 & 0 \end{pmatrix}, \ B = \begin{pmatrix} 0 \\ 0 \\ \vdots \\ 0 \\ 1 \end{pmatrix}, \ C = \begin{pmatrix} 1 \\ 0 \\ \vdots \\ 0 \\ 0 \end{pmatrix}^T.$$

According to the relative degree, three cases of linearized systems (3) must be considered.

Table 3. Vertex values of $g(i_1,i_2)$ in the two dimensional case.

$x_2 \setminus x_1$	$\cdots$	$d_1(\sigma_1)$	$d_1(\sigma_1+1)$	$\cdots$
$\vdots$		$\vdots$	$\vdots$	
$d_2(\sigma_2)$	$\cdots$	$g(\sigma_1,\sigma_2)$	$g(\sigma_1+1,\sigma_2)$	$\cdots$
$d_2(\sigma_2+1)$	$\cdots$	$g(\sigma_1,\sigma_2+1)$	$g(\sigma_1+1,\sigma_2+1)$	$\cdots$
$\vdots$		$\vdots$	$\vdots$	

Table 4. Vertex values of $h(i_1,i_2)$ in the two dimensional case.

$x_2 \setminus x_1$	$\cdots$	$d_1(\sigma_1)$	$d_1(\sigma_1+1)$	$\cdots$
$\vdots$		$\vdots$	$\vdots$	
$d_2(\sigma_2)$	$\cdots$	$h(\sigma_1,\sigma_2)$	$h(\sigma_1+1,\sigma_2)$	$\cdots$
$d_2(\sigma_2+1)$	$\cdots$	$h(\sigma_1,\sigma_2+1)$	$h(\sigma_1+1,\sigma_2+1)$	$\cdots$
$\vdots$		$\vdots$	$\vdots$	

- Relative degree: $\rho = n$

  In this case, the state vector of the input-output linearized system is $\xi = (h,\ L_f h,\ \ldots,\ L_f^{\rho-1}h)^T$. The state vector z should necessarily be a diffeomorphism.

- Relative degree: $\rho < n$

  This is an unobservable state ($n-\rho$ dimensions). It is necessary to consider the zero dynamics of the unobservable state μ. The state vector z should necessarily be a diffeomorphism. $z = \left(\xi,\ \mu\right)^T$, $\xi \in \Re^\rho$, $\mu \in \Re^{n-\rho}$,

  $$\dot{\mu}(\xi,\mu) = \zeta_1(\xi,\mu) + \zeta_2(\xi,\mu)v.$$

  $\dot{\mu}(0,\mu)$ is characterized by zero dynamics.

- In the case of $L_g L_f^i h = 0, \forall i$, the proposed approach cannot be applied.

When the relative degree $\rho \le n$, the input-output linearizing controller is

$$u = \alpha + \beta v, \quad \ldots\ldots\ldots\ldots\ldots\ldots \quad (4)$$

where

$$\alpha = \frac{-L_f^\rho h}{L_g L_f^{\rho-1} h}, \quad \beta = \frac{1}{L_g L_f^{\rho-1} h}.$$

Hereafter, we assume that the relative degree is n (full). The stabilizing linear controller $v = -K\xi$ of the linearized system (3) can be obtained so that the transfer function $G = C(sI-A)^{-1}B$ is Hurwitz.

3.2. Robust PML Controller

It is necessary to design a robust controller, as the PML model is a nonlinear approximation. We designed a robust PML controller [15] for the PML system using the robust feedback linearization method [16]. Consider the following linearized system around an operating point:

$$\begin{cases} \dot{\xi}_r = A_r\xi_r + B_r v_r, \\ y = C_r\xi_r, \end{cases} \quad \ldots\ldots\ldots\ldots \quad (5)$$

where $A_r = \partial f(0)/\partial x$ and $B_r = g(0)$. The distributions $G_0, G_1, \ldots, G_{n-1}$ are defined as

$$\begin{aligned} G_0 &= \quad\ \ \text{span}\{g_1, g_2, \ldots, g_m\}, \\ G_1 &= \text{span}\{g_1, \ldots, g_m, ad_f g_1, \ldots, ad_f g_m\}, \\ &\vdots \\ G_i &= \text{span}\{ad_f^k g_j : 0 \le k \le i, 1 \le j \le m\}, \end{aligned}$$

for $i = 0, 1, \ldots, n-1$.

Proposition 3.1: If the PML system (1) satisfies the following conditions [16],

1. Distribution G_i has a constant dimension near $x = 0$ for $0 \le i \le n-1$,
2. Distribution G_{n-1} has a dimension n,
3. Distribution G_i is the involutive for $0 \le i \le n-2$,

then the robust controller (6) in [15] can be derived as

$$u_r = \alpha_r + \beta_r v_r \quad \ldots\ldots\ldots\ldots\ldots\ldots \quad (6)$$

and the coordinate transformation vector ξ_r is defined by

$$\alpha_r = \alpha + \beta L T^{-1}\xi,\ \beta_r = \beta R^{-1},$$
$$\xi_r = T^{-1}\xi,$$

where $\xi = (h,\ L_f h,\ \ldots,\ L_f^{\rho-1}h)^T$ and

$$L = -L_g L_f^{\rho-1} h \left.\frac{\partial \alpha}{\partial x}\right|_{x=0}, \quad T = \left.\frac{\partial \xi}{\partial x}\right|_{x=0},$$
$$R = \frac{1}{L_g L_f^{\rho-1} h}.$$

The PML system (1) is transformed into the system (5). The linear controller $v_r = -K_r\xi_r$ can be obtained so that the transfer function $G_r = C_r(sI - A_r)^{-1}B_r$ is Hurwitz.

3.3. Tracking PML Controller

We show a tracking control [17] for PML systems. Consider the following reference signal model

$$\begin{cases} \dot{x}_t = f_t, \\ y_t = h_t. \end{cases} \quad \ldots\ldots\ldots\ldots\ldots\ldots \quad (7)$$

where f_t is assumed to be sufficiently smooth in a domain $D \in R^n$ and the output is defined in $C^\rho([0,\infty])$. The controller is designed to make the error signal $\varepsilon = y - y_t \to 0$ as $t \to \infty$. The control object minimizes the difference between the outputs y and y_t. The time derivative of ε is

$$\dot{\varepsilon} = \dot{y} - \dot{y}_t = L_f h + L_g h u - L_{f_t} h_t.$$

If $L_g h = 0$, then we obtain

$$\dot{\varepsilon} = L_f h - L_{f_t} h_t.$$

We continue to calculate the following derivative.

$$\ddot{\varepsilon} = \ddot{y} - \ddot{y}_t = L_f^2 h + L_g L_f h u - L_{f_t}^2 h_t.$$

If $L_g L_f h \neq 0$, then we repeat this calculation until the controller u appears. Finally, we obtain

$$\varepsilon^{(\rho)} = L_f^\rho h + L_g^{\rho-1} L_f h u - L_{f_t}^\rho h_t,$$
$$L_g^{\rho-1} L_f h \neq 0.$$

We set the linearizing coordinate vector

$$\xi_t = \begin{pmatrix} \varepsilon_1 & \varepsilon_2 & \cdots & \varepsilon_\rho \end{pmatrix}^T.$$

Then, the linearized system is $\dot{\xi}_t = A\xi_t + Bv_t$, where A and B are the same as Eq. (3),

$$\begin{aligned} \varepsilon_1 &= \varepsilon = h - h_t, \\ \varepsilon_2 &= \dot{\varepsilon} = L_f h - L_{f_t} h_t, \\ &\vdots \\ \varepsilon_\rho &= \varepsilon^{(\rho-1)} = L_f^{\rho-1} h - L_{f_t}^{\rho-1} h_t, \\ v_t &= \varepsilon^{(\rho)} = L_f^\rho h - L_{f_t}^\rho h_t + L_g L_f^{\rho-1} h u \end{aligned}$$

and $v_t = -K_t\xi_t$ is a linear controller of the linearized system. The model following the controller is obtained as

$$u_t = \alpha_t + \beta_t v_t, \quad \ldots\ldots\ldots\ldots\ldots\ldots \quad (8)$$

where

$$\alpha_t = \frac{-L_f^\rho h + L_{f_t}^\rho h_t}{L_g L_f^{\rho-1} h}, \quad \beta_t = \frac{1}{L_g L_f^{\rho-1} h}.$$

3.4. Observer for PML Systems

We propose an observer of the PML system (1) based on the observer linearization problem [14]. If there exists a coordinate transformation $\zeta = \varphi(x)$ such that the PML system (1) can be transformed into the following system:

$$\begin{aligned} \dot{\zeta} &= A_o \zeta + k + ru, \\ y &= C_o \zeta \end{aligned}$$

with (C_o, A_o) observable and $k, r : R \to R^n$, then it would be possible to build a full-order state observer [11]

$$\begin{aligned} \dot{\hat{\zeta}} &= A_o \hat{\zeta} + k + ru + H(\hat{y} - y), \\ \hat{y} &= C_o \hat{\zeta}, \end{aligned} \quad \ldots\ldots (9)$$

where

$$A_o = \begin{pmatrix} 0 & 0 & \cdots & 0 & 0 \\ 1 & 0 & \cdots & 0 & 0 \\ 0 & 1 & \ddots & \vdots & \vdots \\ \vdots & \ddots & \ddots & 0 & 0 \\ 0 & \cdots & 0 & 1 & 0 \end{pmatrix}, \; C_o = \begin{pmatrix} 0 \\ 0 \\ \vdots \\ 0 \\ 1 \end{pmatrix}^T,$$

and H is the observer gain. The estimation error $e = \hat{\zeta} - \zeta$ satisfies the linear differential equation

$$\dot{e} = (A_o + HC_o)e. \quad \ldots\ldots (10)$$

The estimation state is $\hat{x} = \varphi^{-1}(\hat{\zeta})$. This problem is referred to as the observer linearization problem. The following theorem provides a necessary and sufficient condition for the solution of the observer linearization problem.

Theorem 3.1: The observer linearization problem [14] is solvable if and only if there exists a neighborhood V of an initial condition x_0 that satisfies the following two conditions.

1. $\dim\left(\mathrm{span}\{dh, dL_f h, \ldots, dL_f^{n-1}h\}\right) = n$, where $\forall x \in V$ and d indicates a time derivative.
2. $[ad_f^i \tau, ad_f^j \tau] = 0$, where $0 \le i \le n-1$, $0 \le j \le n-1$, $x \in V$ and $[\,]$ indicates a Lie bracket. The vector field τ satisfies

$$\left(dh, dL_f h, \ldots, dL_f^{n-1}h\right)^T \tau = (0, \ldots, 0, 1)^T.$$

If the PML system (1) is observer linearizable there exists a coordinate transformation φ that satisfies the following condition.

$$L_{(-1)^{j-1} ad_f^{j-1}\tau} \varphi_i = \begin{cases} 0, & i \neq j, \\ 1, & i = j. \end{cases} \quad \ldots\ldots (11)$$

A coordinate transformation can be constructed as $\zeta = \varphi = (\varphi_1, \varphi_2, \ldots, \varphi_n)^T$.

3.5. Observer-Based PML Controller Designs

This paper proposes observer-based PML controllers. We denote several observer-based PML controllers. It is also necessary to construct an observer gain H such that the system (10) is Hurwitz.

3.5.1. Observer-Based PML Controller

Substituting the estimation state $\hat{x} = \varphi^{-1}(\hat{\zeta})$ into the controller (4), the observer-based PML controller can be designed as

$$u(\hat{x}) = \alpha(\hat{x}) + \beta(\hat{x})v, \quad \ldots\ldots (12)$$

where $v = -K\hat{\xi}$ and $\hat{\xi} = (h(\hat{x}), L_f h(\hat{x}), \ldots, L_f^{\rho-1} h(\hat{x}))^T$.

3.5.2. Observer-Based Robust PML Controller

Substituting the estimation state $\hat{x} = \varphi^{-1}(\hat{\zeta})$ into the controller (6), the robust observer-based PML controller can be designed as

$$u_r(\hat{x}) = \alpha_r(\hat{x}) + \beta_r(\hat{x})v_r, \quad \ldots\ldots (13)$$

where $v_r = -K_r \hat{\xi}_r$ and $\hat{\xi}_r = T^{-1}\hat{\xi}$.

3.5.3. Observer-Based Tracking PML Controller

Substituting the estimation state $\hat{x} = \varphi^{-1}(\hat{\zeta})$ into the controller (8), the controller can be designed as

$$u_t(\hat{x}) = \alpha_t(\hat{x}) + \beta_t(\hat{x})v_t, \quad \ldots\ldots (14)$$

where $v_t = -K_t \hat{\xi}_t$ and $\hat{\xi}_t = (h(\hat{x}) - h_r, L_f h(\hat{x}) - L_{f_r} h_r, \ldots, L_f^{\rho-1} h(\hat{x}) - L_{f_r}^{\rho-1} h_r)^T$.

4. Observers and Controllers for Nonlinear Systems

4.1. Two Dimensional Nonlinear System

Consider a two dimensional nonlinear system as follows:

$$\begin{cases} \dot{x} = f + gu, \\ y = h, \end{cases}$$

where $f = \begin{pmatrix} \sin x_2 & -x_1^2 \end{pmatrix}^T$, $g = \begin{pmatrix} 0 & 1 \end{pmatrix}^T$, and $h = x_1$. The feedback linearizing controller is calculated as

$$u = \frac{-L_f h + v}{L_g L_f h} = x_1^2 + \frac{1}{\cos x_2} v. \quad \ldots\ldots (15)$$

The controller cannot be defined outside $-\pi/2 < x_2 < \pi/2$, as the relative degree is not defined for $x_2 = \pm\pi/2$.

The state space is divided into the regions $x_1 \in \{d_1(\sigma_1),\ d_1(\sigma_1+1)\}$ and $x_2 \in \{d_2(\sigma_2),\ d_2(\sigma_2+1)\}$ with respect to the nonlinear terms $\sin x_2$ and x_1^2, respectively. The PML model is constructed as

$$\dot{x} = \begin{pmatrix} \omega_2^{\sigma_2} \sin d_2(\sigma_2) + \omega_2^{\sigma_2+1} \sin d_2(\sigma_2+1) \\ -\omega_1^{\sigma_1} d_1(\sigma_1)^2 - \omega_1^{\sigma_1+1} d_1(\sigma_1+1)^2 \end{pmatrix} + \begin{pmatrix} 0 \\ 1 \end{pmatrix} u,$$

$$y = x_1.$$

Using the same method as the controller (15), the PML controller is calculated as

$$u = (d_1(\sigma_1) + d_1(\sigma_1+1))x_1 - d_1(\sigma_1)d_1(\sigma_1+1) + \frac{d_2(\sigma_2+1) - d_2(\sigma_2)}{\sin d_2(\sigma_2+1) - \sin d_2(\sigma_2)} v.$$

Dividing the vertices $d_2(\sigma_2+1)$ and $d_2(\sigma_2)$ so that $\sin d_2(\sigma_2+1) \neq \sin d_2(\sigma_2)$, there exists a controller outside the bound $-\pi/2 < x_2 < \pi/2$, as the denominator of the controller is not 0.

4.2. Ball and Beam System

The dynamics of a ball and beam (BAB) system [18] is given by

$$\begin{cases} 0 = \ddot{r} + G\sin\theta - r\dot{\theta}^2, \\ \upsilon = (Mr^2 + J)\ddot{\theta} + 2Mr\dot{r}\dot{\theta} + MGr\cos\theta, \end{cases} \quad \ldots (16)$$

where J is the moment of inertia of the beam, M is the mass of the ball, G is the acceleration of gravity, θ is the angle of the beam, r is the position of the ball, and υ is the torque applied to the beam. Using the invertible transformation

$$\upsilon = 2Mr\dot{r}\dot{\theta} + MGr\cos\theta + (Mr^2 + J)u \quad \ldots (17)$$

to define a new input variable u, the system is expressed as

$$\begin{cases} \dot{x} = \begin{pmatrix} x_2 \\ x_1 x_4^2 - G\sin x_3 \\ x_4 \\ 0 \end{pmatrix} + \begin{pmatrix} 0 \\ 0 \\ 0 \\ 1 \end{pmatrix} u, \\ y = x_1, \end{cases} \quad \ldots (18)$$

where $x = (x_1, x_2, x_3, x_4)^T = (r, \dot{r}, \theta, \dot{\theta})$.

4.2.1. PML Model for BAB System

We construct a PML model of the BAB system (18). The nonlinear terms $x_1x_4^2$ and $\sin x_3$ of the BAB system are transformed into PML model representations. The variables x_1, x_3, and x_4 are divided by m_1 vertices, $x_1 \in \{d_1(1), \ldots, d_1(m_1)\}$, m_3 vertices, $x_3 \in \{d_3(1), \ldots, d_3(m_3)\}$ and m_4 vertices, $x_4 \in \{d_4(1), \ldots, d_4(m_4)\}$, respectively. The PML model can be expressed as

$$\begin{cases} \dot{x} = f + gu = \begin{pmatrix} x_2 \\ f_2(x_1, x_3, x_4) \\ x_4 \\ 0 \end{pmatrix} + \begin{pmatrix} 0 \\ 0 \\ 0 \\ 1 \end{pmatrix} u, \\ y = h = x_1, \end{cases} \quad \ldots (19)$$

where $x \in R_{\sigma_1\sigma_2\sigma_3\sigma_4} \equiv [d_1(\sigma_1), d_1(\sigma_1+1)] \times [d_2(\sigma_2), d_2(\sigma_2+1)] \times [d_3(\sigma_3), d_3(\sigma_3+1)] \times [d_4(\sigma_4), d_4(\sigma_4+1)]$,

$$\begin{aligned} f_2(x_1, x_3, x_4) &= f_2^1(x_1, x_4) + f_2^2(x_3), \\ f_2^1(x_1, x_4) &= \sum_{i_1=\sigma_1}^{\sigma_1+1} \sum_{i_4=\sigma_4}^{\sigma_4+1} w_1^{i_1}(x_1) w_4^{i_4}(x_4) d_1(i_1) d_4(i_4)^2, \\ f_2^2(x_3) &= \sum_{i_3=\sigma_3}^{\sigma_3+1} w_3^{i_3}(x_3)(-G\sin d_3(i_3)), \\ \omega_1^{\sigma_1}(x_1) &= \frac{(d_1(\sigma_1+1) - x_1)}{(d_1(\sigma_1+1) - d_1(\sigma_1))}, \\ \omega_1^{\sigma_1+1}(x_1) &= \frac{(x_1 - d_1(\sigma_1))}{(d_1(\sigma_1+1) - d_1(\sigma_1))}, \\ \omega_3^{\sigma_3}(x_3) &= \frac{(d_3(\sigma_3+1) - x_3)}{(d_3(\sigma_3+1) - d_3(\sigma_3))}, \\ \omega_3^{\sigma_3+1}(x_3) &= \frac{(x_3 - d_3(\sigma_3))}{(d_3(\sigma_3+1) - d_3(\sigma_3))}, \\ \omega_4^{\sigma_3}(x_4) &= \frac{(d_4(\sigma_3+1) - x_4)}{(d_4(\sigma_3+1) - d_4(\sigma_3))}, \\ \omega_4^{\sigma_4+1}(x_4) &= \frac{(x_4 - d_4(\sigma_4))}{(d_4(\sigma_4+1) - d_4(\sigma_4))}, \end{aligned}$$

σ_1, σ_3, and σ_4 are integers: $-\infty < \sigma_1, \sigma_3, \sigma_4 < \infty$, $d_1(\sigma_1) < d_1(\sigma_1+1)$, $d_3(\sigma_3) < d_3(\sigma_3+1)$ and $d_4(\sigma_4) < d_4(\sigma_4+1)$.

Note that the trigonometric functions of the BAB system (18) are smooth functions and are of class C^∞. The PML models are not of class C^∞. In the BAB system control, we must calculate the fourth derivatives of the output y. Thus, the derivative PML models lose some dynamics. In this study, we design a robust piecewise controller as a countermeasure for the approximation error of the PML model method.

4.2.2. PML Controller for BAB System

We define the output as $y = x_1$ in $x \in R_{\sigma_1\sigma_2\sigma_3\sigma_4}$, and the time derivative of y is calculated as $\dot{y} = L_f h = x_2$. The time derivative of y does not contain the control inputs u. We calculate the time derivative of $\dot{y}$ as follows:

$$\begin{aligned} \ddot{y} = L_f^2 h &= f_2(x_1, x_3, x_4) \\ &= \sum_{i_1=\sigma_1}^{\sigma_1+1} \sum_{i_4=\sigma_4}^{\sigma_4+1} w_1^{i_1}(x_1) w_4^{i_4}(x_4) d_1(i_1) d_4(i_4)^2 \\ &\quad + \sum_{i_3=\sigma_3}^{\sigma_3+1} w_3^{i_3}(x_3)(-G\sin d_3(i_3)). \end{aligned}$$

The time derivative of $\dot{y}$ also does not contain the control inputs u. We continue to calculate the time derivative of $\ddot{y}$. We obtain

$$\begin{aligned} y^{(3)} &= L_f^3 h + L_g L_f^2 h u \\ &= \frac{\partial f_2^1(x_1, x_4)}{\partial x_1} x_2 + \frac{\partial f_2^2(x_3)}{\partial x_3} x_4 + \frac{\partial f_2^1(x_1, x_4)}{\partial x_4} u. \end{aligned} \quad \ldots (20)$$

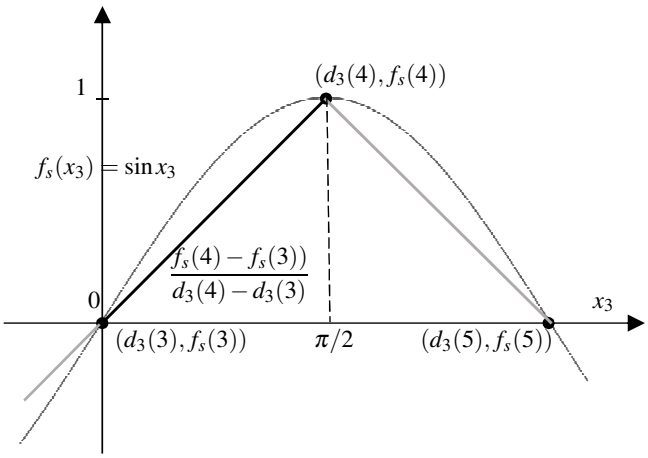

Fig. 2. PML modeling ($d_3(3) = 0$, $d_3(4) = \pi/2$, $d_3(5) = \pi$).

The piecewise controller u derived from Eq. (20) cannot be defined at $x_1 = 0$ or $x_4 = 0$. In this study, we consider the following approximate feedback linearization [14].

$$y^{(3)} \equiv L_f^3 h = \frac{\partial f_2^2(x_3)}{\partial x_3} x_4 = \frac{-G \sin d_3(\sigma_3+1) + G \sin d_3(\sigma_3)}{d_3(\sigma_3+1) - d_3(\sigma_3)} x_4.$$

We continue to calculate the time derivative of $y^{(3)}$. We obtain

$$y^{(4)} = L_g L_f^3 h u = \frac{-G \sin d_3(\sigma_3+1) + G \sin d_3(\sigma_3)}{d_3(\sigma_3+1) - d_3(\sigma_3)} u.$$

The stabilizing controller of Eq. (19) is designed as

$$u = \alpha + \beta\mu, \quad \ldots \quad (21)$$

where

$$\alpha = -\frac{L_f^4 h}{L_g L_f^3 h}, \quad \beta = \frac{1}{L_g L_f^3 h},$$

and $\mu = -F\xi$ is the linear controller of the following linear system (22).

$$\begin{cases} \dot{\xi} = A\xi + B\mu, \\ y = C\xi, \end{cases} \quad \ldots \quad (22)$$

where $\xi = (h,\ L_f h,\ L_f^2 h,\ L_f^3 h)^T$; A, B, and C are the matrices of the Brunovsky canonical form. If $f_s(i) \neq f_s(i+1)$ and $d_3(i) \neq d_3(i+1)$, $i = 1, \ldots, m$, there exists a stabilizing controller (21) of the BAB system (19) as $\det(L_{g_p} L_{f_p}^3 h_p) \neq 0$. Thus, we must construct the PML model of the BAB system such that $f_s(i) \neq f_s(i+1)$ and $d_3(i) \neq d_3(i+1)$, where $i = 1, \ldots, m$ (see **Fig. 2**).

Subsequently, we consider the PML model of the torque (17).

$$\upsilon = \upsilon_1 + \upsilon_2 + \upsilon_3 u, \quad \ldots \quad (23)$$

where

$$\upsilon_1 = \sum_{i_1=\sigma_1}^{\sigma_1+1} \sum_{i_2=\sigma_2}^{\sigma_2+1} \sum_{i_4=\sigma_4}^{\sigma_4+1} \omega_1^{i_1}(x_1)\omega_2^{i_2}(x_2)\omega_4^{i_4}(x_4) \times 2Md_1(i_1)d_2(i_2)d_4(i_4),$$

$$\upsilon_2 = \sum_{i_1=\sigma_1}^{\sigma_1+1} \sum_{i_3=\sigma_3}^{\sigma_3+1} \omega_1^{i_1}(x_1)\omega_3^{i_3}(x_3) MGd_1(i_1)\cos d_3(i_3),$$

$$\upsilon_3 = \sum_{i_1=\sigma_1}^{\sigma_1+1} \omega_1^{i_1}(x_1) Md_1(i_1)^2 + J.$$

Finally, we obtain the torque controller applied to the beam when the controller (21) is substituted into the torque controller (23).

4.2.3. Robust PML Controller for BAB System

The PML model is a nonlinear approximation. Therefore it is necessary to design a robust controller. We design a robust PML controller for the piecewise multilinear model via feedback linearization. We design the robust controller based on the following tangent linearized system around an operating point.

$$\dot{\xi}_r = A_r \xi_r + B_r v_r, \quad \ldots \quad (24)$$

where $A_r = \partial f(0)/\partial x$ and $B_r = g(0)$. The PML system (19) satisfies the conditions in Proposition 3.1. Then under the controller

$$u_r = \alpha_r + \beta_r v_r \quad \ldots \quad (25)$$

and the coordinate transformation vector ξ_r defined by

$$\alpha_r = \alpha + \beta L T^{-1}, \quad \beta_r = \beta R^{-1}, \quad \xi_r = T^{-1}\xi,$$

where $\xi = (h,\ L_f h,\ \ldots,\ L_f^{\rho-1} h)^T$, $R = 1/(L_g L_f^3 h)$,

$$L = -L_g L_f^3 h \left.\frac{\partial \alpha}{\partial x}\right|_{x=0}, \quad T = \left.\frac{\partial \xi}{\partial x}\right|_{x=0},$$

the system (19) is transformed into the system (24). A robust linear controller v_r is substituted into the controller (25). As discussed in the previous section, substituting the controller (25) into Eq. (23), we obtain the torque controller τ.

4.3. TORA System

We consider a translational oscillator with rotating actuator (TORA) system [18] shown in **Fig. 3**, which is one of the benchmark problems for nonlinear control. The TORA system has a cart of mass M connected to a wall with a linear spring (constant k). The cart can oscillate without friction in the horizontal plane. A rotating mass m in the cart is actuated by a motor. The mass is eccentric with a radius of eccentricity e and can be imagined to be a point mass mounted on a massless rotor. The rotating motion of the mass m controls the oscillation of the cart. The motor torque is the control variable. We consider the

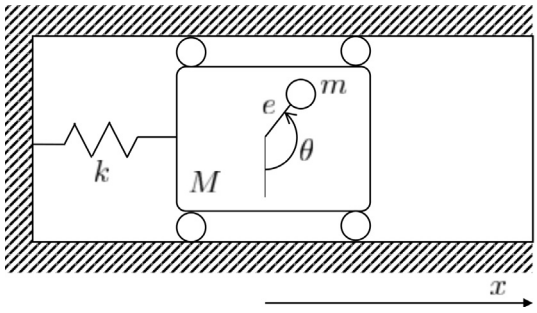

Fig. 3. Kinematic model of the TORA system.

following system [18] after a coordinate transformation as the TORA system.

$$\begin{cases} \dot{x} = f + gu = \begin{pmatrix} x_2 \\ -x_1 + \lambda \sin x_3 \\ x_4 \\ 0 \end{pmatrix} + \begin{pmatrix} 0 \\ 0 \\ 0 \\ 1 \end{pmatrix} u, \\ y = h = x_1, \end{cases} \quad (26)$$

where $x \in R^4$, $y \in R$, and $u \in R$.

4.3.1. PML Model for TORA System

We construct the PML model [11] of the TORA system (26). The state variable x is divided by $m_1 \times m_2 \times m_3 \times m_4$ vertices,

$$x_1 \in \{d_1(1), \ldots, d_1(m_1)\}, x_2 \in \{d_2(1), \ldots, d_2(m_2)\},$$
$$x_3 \in \{d_3(1), \ldots, d_3(m_3)\}, x_4 \in \{d_4(1), \ldots, d_4(m_4)\}.$$

The PML model is expressed as

$$\begin{cases} \dot{x} = f + gu, \\ y = h = x_1, \end{cases} \quad (27)$$

where $x \in R_{\sigma_1 \sigma_2 \sigma_3 \sigma_4}$,

$$f = \sum_{i_1=\sigma_1}^{\sigma_1+1} \sum_{i_2=\sigma_2}^{\sigma_2+1} \sum_{i_3=\sigma_3}^{\sigma_3+1} \sum_{i_4=\sigma_4}^{\sigma_4+1} \omega_1^{i_1}(x_1) \omega_2^{i_2}(x_2) \omega_3^{i_3}(x_3) \omega_4^{i_4}(x_4) \times \begin{pmatrix} d_2(i_2) & -d_1(i_1) + \lambda \sin d_3(i_3) & d_4(i_4) & 0 \end{pmatrix}^T,$$

$$g = \begin{pmatrix} 0 & 0 & 0 & 1 \end{pmatrix}^T,$$

$$\omega_j^{\sigma_j}(x_j) = \frac{d_j(\sigma_j + 1) - x_j}{d_j(\sigma_j + 1) - d_j(\sigma_j)},$$

$$\omega_1^{\sigma_j + 1}(x_j) = \frac{x_j - d_j(\sigma_j)}{d_j(\sigma_j + 1) - d_j(\sigma_j)},$$

$$j = 1, \ldots, 4.$$

The model is observed to be fully parametric and the internal model dynamics is described by a multi-linear interpolation of the vertices: $d_1(i_1)$, $d_2(i_2)$, $d_3(i_3)$, and $d_4(i_4)$. The PML model can be represented by a lookup table (LUT).

Note that the trigonometric functions of the TORA system (26) are smooth functions and are of class C^∞. The PML models are not of class C^∞. In the TORA system control, we must calculate the fourth derivatives of the output y. Thus, the derivative PML models lose some dynamics. However, the PML model-based control for the TORA system can be applied to a wider region compared with the conventional one.

Note that there are some modeling errors because the PML model is a nonlinear approximation. In the proposed method, the vertices $d_i(j)$ of an arbitrary number can be set on an arbitrary position of the state space. Therefore, the approximated error can be adjusted easily.

4.3.2. Nonlinear Controller for TORA System

We show the controller of the TORA system (26) via feedback linearization [14]. We calculate the time derivatives of the output y until the input u appears. Then the feedback linearizing controller is obtained as

$$u = \frac{-x_1 + \lambda \sin x_3 + \lambda x_4^2 \sin x_3}{\lambda \cos x_3} + \frac{1}{\lambda \cos x_3} \mu, \quad . \quad (28)$$

where μ is the linear controller for the linearized system:

$$\begin{cases} \dot{\xi} = A\xi + B\mu, \\ y = C\xi, \\ \xi = (h, L_f h, L_f^2 h, L_f^3 h)^T, \end{cases}$$

$$A = \begin{pmatrix} 0 & 1 & 0 & 0 \\ 0 & 0 & 1 & 0 \\ 0 & 0 & 0 & 1 \\ 0 & 0 & 0 & 0 \end{pmatrix}, B = \begin{pmatrix} 0 \\ 0 \\ 0 \\ 1 \end{pmatrix}, C = \begin{pmatrix} 1 \\ 0 \\ 0 \\ 0 \end{pmatrix}^T. \quad (29)$$

However, the controller (28) is only well defined at $-\pi/2 < x_3 < \pi/2$ because the denominator of the controller is $\lambda \cos x_3$. Hence, the rotor of the TORA system can only be rotated at $-\pi/2 < \theta < \pi/2$.

4.3.3. PML Controller for TORA System

The time derivative of the output $y = x_1$ must be calculated until the input u appears. Then, the PML controller [11] of Eq. (27) is designed as

$$u = \frac{-x_1 + \sum_{i_3=\sigma_3}^{\sigma_3+1} \omega_3^{i_3}(x_3) \lambda \sin d_3(i_3)}{\lambda \dfrac{\sin d_3(\sigma_3 + 1) - \sin d_3(\sigma_3)}{d_3(\sigma_3 + 1) - d_3(\sigma_3)}} + \frac{d_3(\sigma_3 + 1) - d_3(\sigma_3)}{\lambda (\sin d_3(\sigma_3 + 1) - \sin d_3(\sigma_3))} v, \quad . \quad . \quad (30)$$

where $v = -K\xi$ is the linear controller of the linear system:

$$\begin{cases} \dot{\xi} = A\xi + Bv, \\ y = C\xi, \\ \xi = (h, L_f h, L_f^2 h, L_f^3 h)^T. \end{cases}$$

The matrix A and the vectors B and C are the same as Eq. (29).

If $\sin d_3(\sigma_3) \neq \sin d_3(\sigma_3 + 1)$ and $d_3(\sigma_3) \neq d_3(\sigma_3 + 1)$, there exists a controller (30) of the TORA system (27) as

$\det(L_g L_f^3 h) \neq 0$. Thus, it is necessary to construct a PML model of the TORA system that satisfies the above conditions. Note that the PML model-based controller (30) can be applied to a wider region compared with the conventional feedback linearized controller.

4.3.4. Robust PML Controller for TORA System

The parameters of the linearized system (5) are calculated as

$$A_r = \begin{pmatrix} 0 & 1 & 0 & 0 \\ -1 & 0 & \lambda \dfrac{\sin d_(\sigma_3+1) - \sin d_(\sigma_3)}{d_3(\sigma+1) - d_3(\sigma)} & 0 \\ 0 & 0 & 0 & 1 \\ 0 & 0 & 0 & 0 \end{pmatrix},$$

$$B_r = \begin{pmatrix} 0 \\ 0 \\ 0 \\ 1 \end{pmatrix}.$$

The robust PML controller [15] is designed as

$$u_r = \alpha_r + \beta_r v_r.$$

The coordinate transformation vector is obtained as

$$\xi_r = \begin{pmatrix} x_1 \\ x_2 \\ \displaystyle\sum_{i_3=\sigma_3}^{\sigma_3+1} \omega_3^{i_3}(x_3) \sin d_3(i_3) \\ \dfrac{\sin d_3(\sigma_3+1) - \sin d_3(\sigma_3)}{d_3(\sigma_3+1) - d_3(\sigma_3)} \\ x_4 \end{pmatrix}.$$

4.3.5. Observer for TORA System

The condition 1 of Theorem 3.1 is applied to the original nonlinear system (26).

$$\det\left(dh^T dL_f h^T \ldots dL_f^{n-1} h^T\right)^T = \lambda^2 \cos^2 x_3.$$

Thus, the above matrix is not linear independence at $x_3 \pm \pi/2$. One of the condition 2 is also calculated for the original nonlinear model as follows:

$$\left[ad_f^0 \tau,\ ad_f^3 \tau\right] = \frac{2 \sin x_3}{\lambda^2 \cos^3 x_3}.$$

The above equation is equal to 0 at $x_3 = 0$ and the equation cannot be defined at $x_3 \pm \pi/2$. Therefore, the nonlinear system (26) is not observer linearizable.

4.3.6. PML Observer for TORA System

The condition 1 of Theorem 3.1 is applied to the PML system (27).

$$\det\left(dh^T dL_f h^T \ldots dL_f^{n-1} h^T\right)^T = a \neq 0,$$

where a is a non-negative constant value. The condition 2 of Theorem 3.1 is also applied to the original nonlinear system (27).

$$[ad_f^i \tau, ad_f^j \tau] = 0,$$

where $0 \leq i \leq 3$, $0 \leq j \leq 3$, and $\tau = \begin{pmatrix} 0 & 0 & 0 & 1/a \end{pmatrix}^T$. Therefore, the PML system (27) is observer linearizable. From the condition (11), the coordinate transformation vector is calculated as $\varphi = \begin{pmatrix} ax_4 & ax_3 & x_2 & x_1 \end{pmatrix}^T$.

4.3.7. Observer-Based Tracking PML Controller for TORA System

We design the tracking controller of the TORA system using the PML model. Consider the reference signal model (7). Then, the controller is designed to make the error signal $e_t = y - y_r = h - h_t \to 0$ as $t \to \infty$. The time derivative of the error e is obtained as

$$\dot{e}_t = L_f h - L_{f_t} h_t(x_t).$$

The time derivative is calculated until the input u appears. Subsequently, the PML controller is obtained as

$$u_t = \alpha_t + \beta_t v_t, \quad \ldots\ldots\ldots\ldots\ldots\ldots \quad (31)$$

where

$$\alpha_t = -\frac{L_f^4 h - L_{f_t}^4 h_t(x_t)}{L_g L_f^3 h}, \quad \beta_t = \frac{1}{L_g L_f^3 h}.$$

In Eq. (30), $v_t = -K_t \xi_t$ is the linear controller of the linear system:

$$\begin{cases} \dot{\xi}_t = A\xi_t + Bv, \\ y = C\xi_t, \\ \xi_t = \begin{pmatrix} h - h_t(x_t) \\ L_f h - L_{f_t} h_t(x_t) \\ L_f^2 h - L_{f_t}^2 h_t(x_t) \\ L_f^3 h - L_{f_t}^3 h_t(x_t) \end{pmatrix}. \end{cases}$$

The matrix A and the vectors B and C are the same as Eq. (29).

5. Simulation Results

We show some examples to confirm the feasibility of our proposals. Consider the following nonlinear systems:

5.1. Ball and Beam System

To construct the PML model of the BAB system, the state variables x_1, x_2, x_3, and x_4 of the BAB system (16) are divided by the following vertices

$$x_1 \in \{-3,\ -1.5,\ 0,\ 1.5,\ 3\},\ x_2 \in \{-3,\ -1.5,\ 0,\ 1.5,\ 3\},$$
$$x_3 \in \{-\pi/8,\ -\pi/16,\ 0,\ \pi/16,\ \pi/8\},$$
$$x_4 \in \{-0.4,\ -0.2,\ 0,\ 0.2\ 0.4\}.$$

The initial condition is $x(0) = (1.5,\ 0,\ 0,\ 0)^T$ and the acceleration of gravity $G = 9.81$ m/s^2. The nominal values of the system parameters are as follows: $M = 0.1$ kg and $J = 0.1$ kg·m^2.

The model is observed to be fully parametric and can be represented by an LUT. **Table 5** shows the vertex values of $f_2(x_1, x_3, x_4)$. The internal model dynamics is de-

Table 5. Vertex values of $f_2(x_1, x_3, x_4)$.

		x_4				
x_3	x_1	-0.4	-0.2	0	0.2	0.4
$-\pi/8$	-3	3.274	3.634	3.754	3.634	3.274
	-1.5	3.514	3.694	3.754	3.694	3.514
	0	3.754	3.754	3.754	3.754	3.754
	1.5	3.994	3.814	3.754	3.814	3.994
	3	4.234	3.874	3.754	3.874	4.234
$-\pi/16$	-3	1.434	1.794	1.914	1.794	1.434
	-1.5	1.674	1.854	1.914	1.854	1.674
	0	1.914	1.914	1.914	1.914	1.914
	1.5	2.154	1.974	1.914	1.974	2.154
	3	2.394	2.034	1.914	2.034	2.394
0	-3	-0.480	-0.120	0	-0.120	-0.480
	-1.5	-0.240	-0.060	0	-0.060	-0.240
	0	0	0	0	0	0
	1.5	0.240	0.060	0	0.060	0.240
	3	0.480	0.120	0	0.120	0.480
$\pi/16$	-3	-2.394	-2.034	-1.914	-2.034	-2.394
	-1.5	-2.154	-1.974	-1.914	-1.974	-2.154
	0	-1.914	-1.914	-1.914	-1.914	-1.914
	1.5	-1.674	-1.854	-1.914	-1.854	-1.674
	3	-1.434	-1.794	-1.914	-1.794	-1.434
$\pi/8$	-3	-4.234	-3.874	-3.754	-3.874	-4.234
	-1.5	-3.994	-3.814	-3.754	-3.814	-3.994
	0	-3.754	-3.754	-3.754	-3.754	-3.754
	1.5	-3.514	-3.694	-3.754	-3.694	-3.514
	3	-3.274	-3.634	-3.754	-3.634	-3.274

Table 6. Vertex values of the PML controller ($x_2 = 1.5$).

		x_4				
x_3	x_1	-0.4	-0.2	0	0.2	0.4
$-\pi/8$	-3	0.5244	-0.1085	-0.8498	-1.700	-2.658
	-1.5	-0.1551	-0.4187	-0.7000	-0.9988	-1.315
	0	0.3420	0.2805	0.2189	0.1574	0.0958
	1.5	2.378	2.242	2.123	2.022	1.938
	3	6.316	5.718	5.228	4.847	4.574
$-\pi/16$	-3	-0.5064	-1.145	-1.889	-2.737	-3.689
	-1.5	-0.5228	-0.7874	-1.069	-1.368	-1.683
	0	0.2536	0.1921	0.1305	0.0690	0.0074
	1.5	2.171	2.036	1.917	1.816	1.731
	3	5.579	4.987	4.500	4.116	3.837
0	-3	-1.395	-2.034	-2.777	-3.625	-4.577
	-1.5	-0.8214	-1.086	-1.368	-1.666	-1.982
	0	0.1705	0.1089	0	-0.0142	-0.0757
	1.5	1.929	1.794	1.675	1.574	1.489
	3	4.804	4.212	3.724	3.341	3.062
$\pi/16$	-3	-2.205	-2.838	-3.579	-4.429	-5.387
	-1.5	-1.071	-1.335	-1.616	-1.915	-2.232
	0	0.0859	0.0243	-0.0372	-0.0988	-0.1604
	1.5	1.630	1.493	1.374	1.273	1.189
	3	3.922	3.324	2.834	2.453	2.180
$\pi/8$	-3	-2.869	-3.502	-4.243	-5.093	-6.051
	-1.5	-1.258	-1.522	-1.803	-2.102	-2.418
	0	0.0027	-0.0589	-0.1204	-0.1820	-0.2435
	1.5	1.275	1.139	1.020	0.9189	0.8353
	3	2.923	2.325	1.835	1.454	1.181

scribed by a multi-linear interpolation of the LUT elements (see **Fig. 1**).

We apply the PML controller in **Table 6** and the robust PML controller in **Table 7** to a nominal BAB system (16) and a BAB system with parameter variation in computer simulations. The torque controllers are observed to be fully parametric and can be represented by an LUT. Owing to lack of space, the PML controllers at $x_2 = 1.5$ are only shown in **Tables 6** and **7**. The internal model dynamics is described by a multi-linear interpolation of the LUT elements.

Figure 4 shows the control responses $x_1, \ldots, x_4$ of the nominal BAB system. In **Figs. 5** and **6**, we consider the parameter variations with respect to the mass M of the ball. **Figs. 5** and **6** show the control responses of the BAB systems with parameter variations (the masses of the ball: $M' = 1.1M$ and $M' = 1.2M$). The results confirm the feasibility of the proposed robust PML controller for the BAB system with parameter variations.

Table 7. Vertex values of the robust PML controller ($x_2 = 1.5$).

		x_4				
x_3	x_1	-0.4	-0.2	0	0.2	0.4
$-\pi/8$	-3	4.137	3.546	2.489	0.9751	-0.7469
	-1.5	1.528	1.223	0.8205	0.3242	-0.1855
	0	1.016	0.9254	0.8208	0.7041	0.6000
	1.5	5.079	4.792	4.514	4.253	4.086
	3	16.190	14.96	13.93	13.11	12.75
$-\pi/16$	-3	1.379	0.7393	-0.3320	-1.824	-3.549
	-1.5	0.6004	0.2811	-0.1255	-0.6153	-1.127
	0	0.7563	0.6612	0.5554	0.4407	0.3355
	1.5	4.315	4.016	3.736	3.480	3.308
	3	13.75	12.48	11.44	10.64	10.26
0	-3	-1.295	-1.962	-3.033	-4.499	-6.223
	-1.5	-0.2788	-0.6066	-1.013	-1.494	-2.006
	0	0.4944	0.3967	0	0.1788	0.0736
	1.5	3.493	3.185	2.905	2.657	2.485
	3	11.18	9.896	8.853	8.076	7.696
$\pi/16$	-3	-3.919	-4.591	-5.649	-7.081	-8.803
	-1.5	-1.120	-1.451	-1.853	-2.323	-2.833
	0	0.2275	0.1284	0.0238	-0.0848	-0.1889
	1.5	2.599	2.285	2.008	1.772	1.606
	3	8.470	7.159	6.124	5.386	5.026
$\pi/8$	-3	-6.313	-7.012	-8.069	-9.475	-11.20
	-1.5	-1.869	-2.208	-2.611	-3.072	-3.582
	0	-0.0286	-0.1304	-0.2350	-0.3409	-0.4450
	1.5	1.683	1.361	1.083	0.8562	0.6893
	3	5.741	4.404	3.369	2.657	2.297

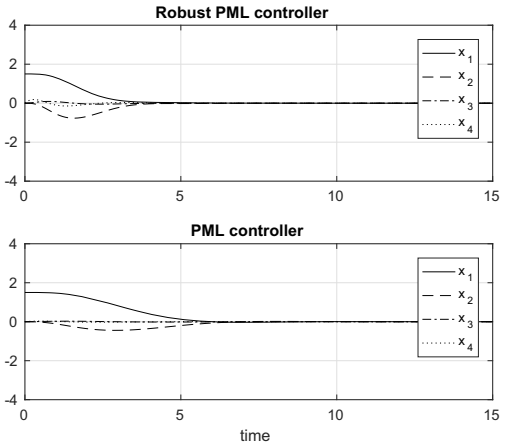

Fig. 4. State responses of the nominal BAB system.

5.2. TORA System

The observer-based PML controllers (12) and (13) are applied to the TORA system (26) in computer simulation. In the simulations, the state variables x_1, x_2, x_3, and x_4 of the TORA system are divided by the following vertices:

$$x_1 \in \{-2.0,\ 0,\ 2.0\},\ x_2 \in \{-2.0,\ 0,\ 2.0\},$$
$$x_3 \in \{-\pi, -7\pi/8, \ldots, \pi\},\ x_4 \in \{-2.0,\ 0,\ 2.0\}.$$

The parameter λ is 0.5 and the initial condition is $x(0) = (0.5,\ 0,\ 0,\ 0)^T$.

Figures 7, **8**, and **9** show the simulation re-

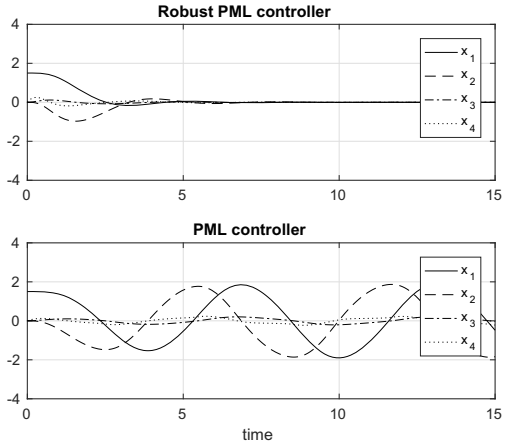

Fig. 5. State responses of the BAB system with parameter variation ($M' = 1.1M$).

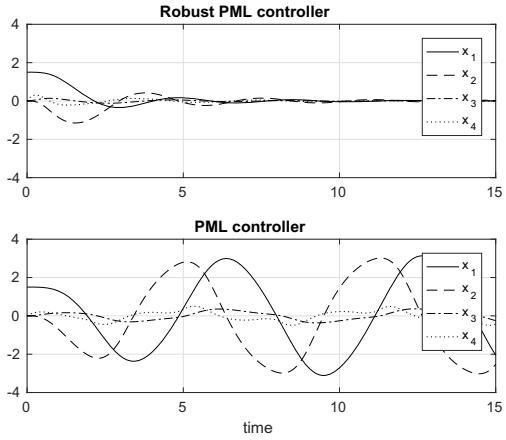

Fig. 6. State responses of the BAB system with parameter variation ($M' = 1.2M$).

sults obtained using the observer-based PML controller (12), where the feedback gain $K = (1.000,\ 3.078,\ 4.236,\ 3.078)$ and the observer gain $H = (1,\ 3.078,\ 4.236,\ 3.078)^T$ such that the linearized and observer systems are stable, respectively. These gains are designed using linear quadratic Gaussian (LQG) methods for the linearized systems. These figures show that the controller (12) cannot stabilize the TORA system (26) with the estimation errors $e = \hat{\zeta} - \zeta$ of the observer (9).

Figures 10, **11**, and **12** show the simulation results obtained using the robust observer-based PML controller (13), where the feedback and observer gains (K and H) are, respectively, the same as those of the observer-based PML controller (12). The controller (13) can stabilize the TORA system (26) with the estimation errors $e = \hat{\zeta} - \zeta$ of the observer (9).

The observer-based tracking PML controller (14) is applied to the TORA system (26) in computer simulations. In the simulations, the state variables x_1, x_2, x_3, and x_4

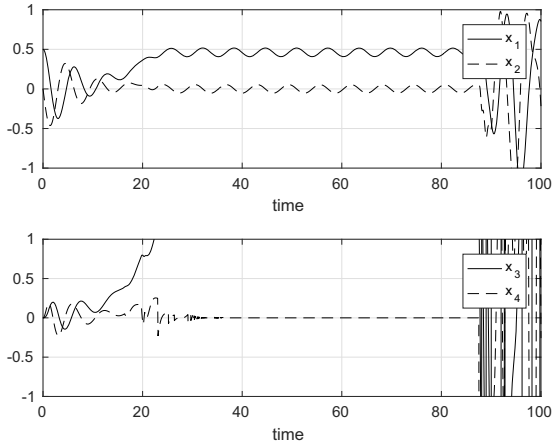

Fig. 7. State responses (x_1, x_2, x_3, and x_4) obtained using the observer-based PML controller (12).

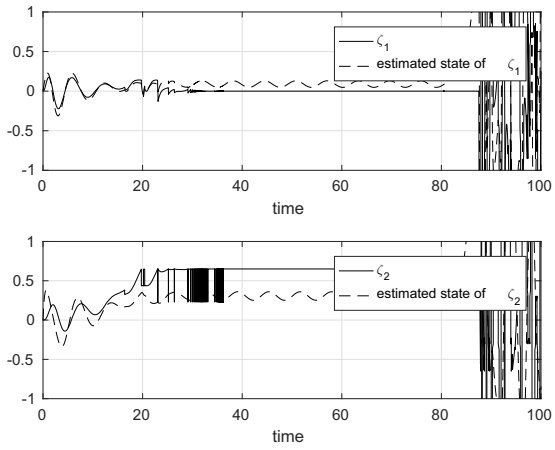

Fig. 8. State responses (ζ_1 and ζ_2) and the estimations obtained using the observer-based PML controller (12).

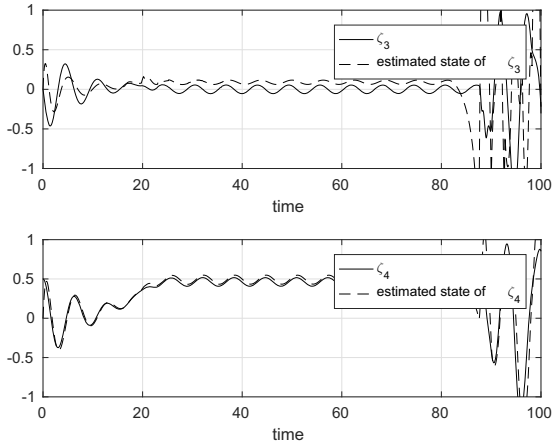

Fig. 9. States responses (ζ_3 and ζ_4) and the estimations obtained using the observer-based PML controller (12).

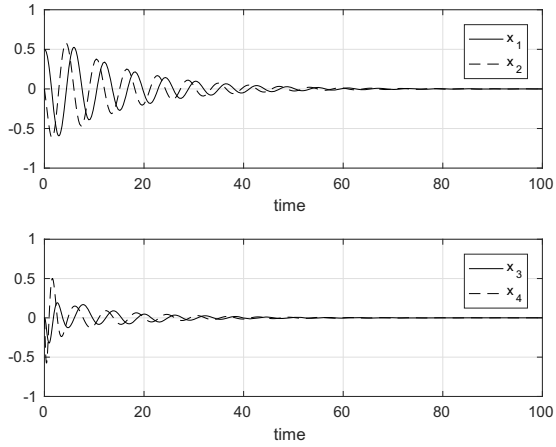

Fig. 10. State responses (x_1, x_2, x_3, and x_4) obtained using the robust observer-based PML controller (14).

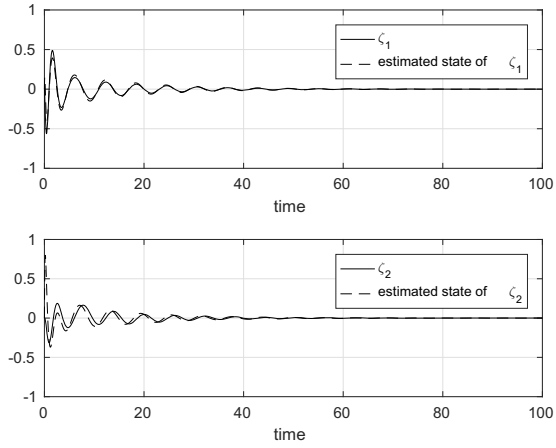

Fig. 11. State responses (ζ_1 and ζ_2) and the estimations obtained using the robust observer-based PML controller (14).

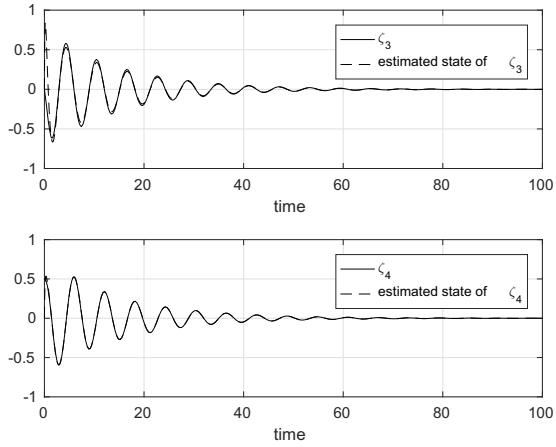

Fig. 12. State responses (ζ_3 and ζ_4) and the estimations obtained using the robust observer-based PML controller (14).

of the TORA system are divided by the same vertices as those in the previous example. The parameter λ and the initial condition $x(0)$ are also, respectively, the same as those in the previous example. We consider the following reference signal model:

$$\begin{cases} \dot{x}_t = a_t \cos t, \\ y_t = h_t = x_t, \end{cases}$$

where $a_t = 0.2$.

Figures 13, **14**, and **15** show the simulation results obtained using the observer-based tracking PML controller (14), where the feedback gain $K_t = (1.000,\ 3.078,\ 4.236,\ 3.078)$ and the observer gain $H = (10.00,\ 25.09,\ 26.47,\ 12.37)^T$ such that the linearized and observer systems are stable, respectively. These gains are designed using LQG methods for the linearized systems.

The PML controller (14) stabilizes the TORA system (26) with the estimation error $e = \hat{\zeta} - \zeta$ and the tracking error $e_t = y - y_r$. In **Fig. 13**, the solid line and the dotted line of the upper figure indicate the control input y and the reference signal y_r, respectively. The solid line of the lower figure indicates the error signal $y - y_r$. In **Figs. 14** and **15**, the solid lines and the dotted lines indicate the state responses (ζ_1, ζ_2, ζ_3, and ζ_4) and the estimated states, respectively.

6. Conclusion

This paper has proposed observer-based piecewise multi-linear controllers for nonlinear systems using piecewise multi-linear models. The piecewise model is a nonlinear approximation and is fully parametric. Feedback linearizations have been applied to stabilize the piecewise multi-linear control system. Observer linearizations are more conservative in modeling errors compared with feedback linearizations. In this paper, we have proposed robust observer designs for piecewise multi-linear systems. In addition, we have designed piecewise multi-linear controllers that combines the robust observer with various performance such as a regulator and a tracking controller. These design methods realize a separation principle that allows an observer and a regulator to be designed separately. Examples have been demonstrated through computer simulation to confirm the feasibility of our proposals. In future work, the proposed methods will be applied to real systems.

References:

[1] E. D. Sontag, "Nonlinear regulation: the piecewise linear approach," IEEE Trans. Autom. Control, Vol.26, No.2, pp. 346-358, doi: 10.1109/TAC.1981.1102596, 1981.

[2] M. Johansson and A. Rantzer, "Computation of piecewise quadratic Lyapunov functions for hybrid systems," IEEE Trans. Autom. Control, Vol.43, No.4, pp. 555-559, doi: 10.1109/9.664157, 1998.

[3] J. Imura and A. van der Schaft, "Characterization of well-posedness of piecewise-linear systems," IEEE Trans. Autom. Control, Vol.45, No.9, pp. 1600-1619, doi: 10.1109/9.880612, 2000.

[4] G. Feng, G. P. Lu, and S. S. Zhou, "An approach to H_∞ controller synthesis of piecewise linear systems," Communications in Infor-

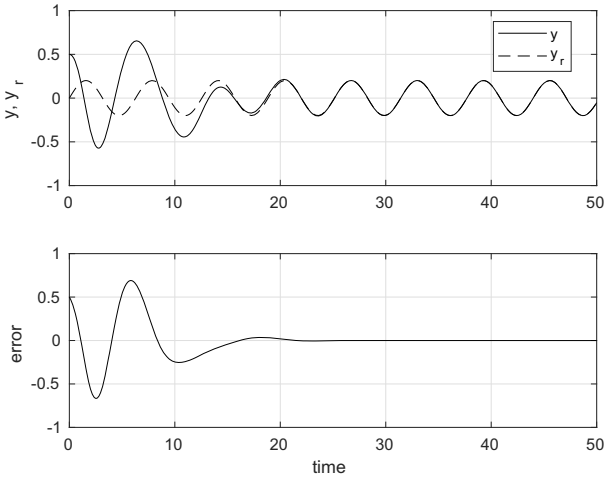

Fig. 13. Control output (y), reference signal (y_r), and the error signal ($y - y_r$).

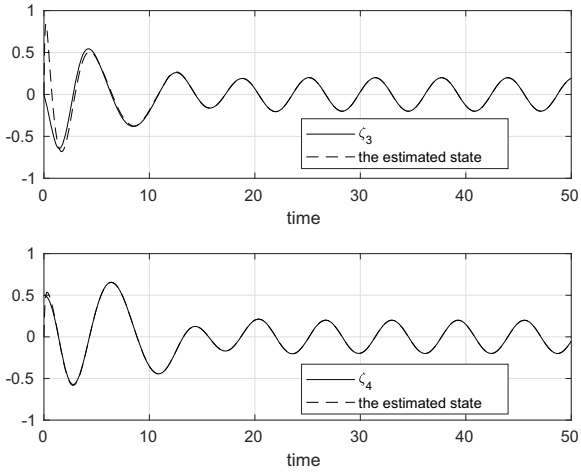

Fig. 15. State responses (ζ_3, ζ_4) and the estimated states.

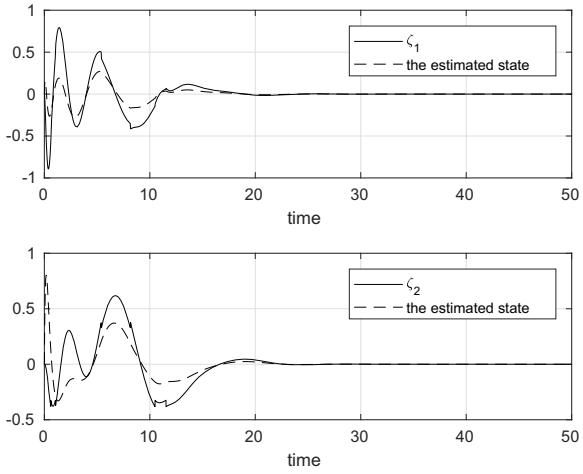

Fig. 14. State responses (ζ_1, ζ_2) and the estimated states.

mation and Systems, Vol.2, No.3, pp. 245-254, doi: 10.4310/CIS.2002.v2.n3.a2, 2002.

[5] M. Sugeno, "On stability of fuzzy systems expressed by fuzzy rules with singleton consequents," IEEE Trans. Fuzzy Syst., Vol.7, No.2, pp. 201-224, doi: 10.1109/91.755401, 1999.

[6] M. Sugeno and T. Taniguchi, "On improvement of stability conditions for continuous Mamdani-like fuzzy systems," IEEE Trans. Systems, Man, and Cybernetics, Part B, Vol.34, No.1, pp. 120-131, doi: 10.1109/TSMCB.2003.809226, 2004.

[7] K.-C. Goh, M. G. Safonov, and G. P. Papavassilopoulos, "A global optimization approach for the BMI problem," Proc. of the 33rd IEEE Conf. on Decision and Control, Vol.3, pp. 2009-2014, doi: 10.1109/CDC.1994.411445, 1994.

[8] T. Taniguchi and M. Sugeno, "Stabilization of Nonlinear Systems with Piecewise Bilinear Models derived from Fuzzy If-Then Rules with Singletons," Proc. of Int. Conf. on Fuzzy Systems, pp. 2926-2931, doi: 10.1109/FUZZY.2010.5584807, 2010.

[9] T. Taniguchi, L. Eciolaza, and M. Sugeno, "Full-Order State Observer Design for Nonlinear Systems Based on Piecewise Bilinear Models," Int. J. of Modeling and Optimization, Vol.4, No.2, pp. 120-125, doi: 10.7763/IJMO.2014.V4.358, 2014.

[10] T. Taniguchi, L. Eciolaza, and M. Sugeno, "Designs of Minimal-Order State Observer and Servo Controller for a Robot Arm Using Piecewise Bilinear Models," Proc. of The 2014 IAENG Int. Multi-Conf. of Engineers and Computer Scientists, 2014.

[11] T. Taniguchi and M. Sugeno, "Robust Observer-Based Piecewise Multi-Linear Controller Design for Nonlinear Systems," Proc. of 2018 Joint 10th Int. Conf. on Soft Computing and Intelligent Systems (SCIS) and 19th Int. Symp. on Advanced Intelligent Systems (ISIS), pp. 902-907, doi: 10.1109/SCIS-ISIS.2018.00149, 2018.

[12] T. Taniguchi, L. Eciolaza, and M. Sugeno, "LUT Controller Design with Piecewise Bilinear Systems Using Estimation of Bounds for Approximation Errors," J. Adv. Comput. Intell. Intell. Inform., Vol.17, No.6, pp. 828-840, doi: 10.20965/jaciii.2013.p0828, 2013.

[13] A. Isidori, "The matching of a prescribed linear input-output behavior in a nonlinear system," IEEE Trans. Autom. Control, Vol.30, No.3, pp. 258-265, doi: 10.1109/TAC.1985.1103939, 1985.

[14] S. Sastry, "Nonlinear Systems," Springer, 1999.

[15] T. Taniguchi and M. Sugeno, "Robust Lookup Table Controller Based on Piecewise Multi-Linear Model for Nonlinear Systems with Parametric Uncertainty," Proc. of 17th Int. Conf. on Information Processing and Management of Uncertainty in Knowledge-Based Systems, pp. 727-738, doi: 10.1007/978-3-319-91479-4_60, 2018.

[16] H. Guillard and H. Bourlès, "Robust feedback linearization," Proc. of 14th Int. Symp. Mathematical Theory of Networks and Systems, pp. 1-6, 2000.

[17] T. Taniguchi, L. Eciolaza, and M. Sugeno, "Look-Up-Table Controller Design for Nonlinear Servo Systems with Piecewise Bilinear Models," Proc. of 2013 IEEE Int. Conf. on Fuzzy Systems (FUZZ-IEEE), doi: 10.1109/FUZZ-IEEE.2013.6622512, 2013.

[18] R. Sepulchre, M. Jankovic, and P. V. Kokotovic, "Constructive Nonlinear Control," Springer, 1997.

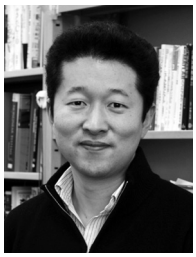

Name:
Tadanari Taniguchi

Affiliation:
Tokai University

Address:
4-1-1 Kitakaname, Hiratsuka, Kanagawa 259-1292, Japan

Brief Biographical History:
1996 Received the B.S. degree in Mechanical Systems Engineering from Kanazawa University
1998 Received the M.S. degree in Mechanical Systems Engineering from Kanazawa University
2001 Received the Ph.D. degree in Mechanical and Control Engineering from University of Electro-Communications
2001-2005 Research Scientist, The Brain Science Institute, RIKEN
2005- IT Education Center, Tokai University
2012- Associate Professor, Tokai University
2015-2016 Visiting Researcher, Université de Valenciennes

Main Works:
- Intelligent Control
- Nonlinear Control Based on Piecewise Models
- Smart Education

Membership in Academic Societies:
- The Institute of Electrical and Electronics Engineers (IEEE)
- Japan Society for Fuzzy Theory and Intelligence Informatics (SOFT)
- The Society of Instrument and Control Engineers (SICE)

Name:
Michio Sugeno

Affiliation:
Tokyo Institute of Technology

Address:
4259 Nagatsuta-cho, Midori-ku, Yokohama, Kanagawa 226-8503 Japan

Brief Biographical History:
1962 Graduated from Department of Physics, The University of Tokyo
1965- Research Associate, Tokyo Institute of Technology
1978- Associate Professor, Tokyo Institute of Technology
1985-2000 Professor, Tokyo Institute of Technology
1991-1993 President, Japan Society for Fuzzy Theory and Systems
1997-1999 President, International Fuzzy Systems Association
2000-2005 Laboratory Head, Brain Science Institute, RIKEN
2000- Emeritus Professor, Tokyo Institute of Technology
2005-2010 Distinguished Visiting Professor, Doshisha University
2010 First Recipient of IEEE CIS Pioneer Award in Fuzzy Systems with Zadeh
2010 Received 2010 IEEE Frank Rosenblatt Award
2010-2015 Emeritus Researcher, European Centre for Soft Computing
2017 Received IEEE SMC 2017 Lotfi A. Zadeh Pioneer Award

Main Works:
- Text Generation Based on Systemic Functional Linguistics
- Ordinal Preference Models Based on S-Integrals
- Nonlinear Control Based on Piecewise Models

Membership in Academic Societies:
- The Institute of Electrical and Electronics Engineers (IEEE)
- Japan Society for Fuzzy Theory and Intelligence Informatics (SOFT)
- Japan Association of Systemic Functional Linguistics (JASFL)